

Simulation-based Machine Learning Training for Brain Anomalies Localization at Microwaves

*Original*

Simulation-based Machine Learning Training for Brain Anomalies Localization at Microwaves / Mariano, Valeria; Casu, Mario R.; Vipiana, Francesca. - ELETTRONICO. - (2022). ((Intervento presentato al convegno 2022 16th European Conference on Antennas and Propagation (EuCAP) tenutosi a Madrid, Spain nel 27 March-1 April 2022 [10.23919/EuCAP53622.2022.9769504].

*Availability:*

This version is available at: 11583/2964071 since: 2022-05-18T14:48:50Z

*Publisher:*

IEEE

*Published*

DOI:10.23919/EuCAP53622.2022.9769504

*Terms of use:*

openAccess

This article is made available under terms and conditions as specified in the corresponding bibliographic description in the repository

*Publisher copyright*

IEEE postprint/Author's Accepted Manuscript

©2022 IEEE. Personal use of this material is permitted. Permission from IEEE must be obtained for all other uses, in any current or future media, including reprinting/republishing this material for advertising or promotional purposes, creating new collecting works, for resale or lists, or reuse of any copyrighted component of this work in other works.

(Article begins on next page)

# Simulation-based Machine Learning Training for Brain Anomalies Localization at Microwaves

Valeria Mariano, Mario R. Casu, Francesca Vipiana  
 Dept. of Electronics and Telecommunication  
 Politecnico di Torino  
 Torino, Italy  
 {valeria\_mariano, mario.casu, francesca.vipiana}@polito.it

**Abstract**—Machine learning enters the world of medical application and, in this paper, it joins microwave imaging technique for brain stroke classification. One of the main challenges in this application is the need of a large amount of data for the machine learning algorithm training that can be performed via measurements or simulations. In this work, we propose to make the algorithm training via simulations based on a linear integral operator that reduces by three orders of magnitude the data generation time with respect to standard full-wave simulations. This method is used here to train the multilayer perceptron algorithm. The data-set is organized in nine classes, related to the presence, the type and the position of the stroke within the brain. We verified that the algorithm metrics (accuracy, recall and precision) reach values close to 1 for each class.

**Index Terms**—Machine learning, brain stroke classification, multilayer perceptron, microwave imaging.

## I. INTRODUCTION

In the last years, machine learning is spreading more and more in different fields, and among them there are several medical applications. In this paper, machine learning is applied to brain stroke classification. Brain stroke is linked to an acute dysfunction of a cardiovascular mechanism and it is localized in a single brain area. The intervention time is a fundamental factor for stroke patient, in fact a short intervention time could avoid death or too extended paralysis.

In this context, microwave imaging technology is proposed as a complementary diagnosis tool to others already available (e.g., magnetic resonance imaging and computerized tomography) thanks to the possibilities of having a portable, non-invasive, low-cost and with a small size system [1]. Machine learning (ML) combined with microwave imaging techniques [2]–[4] could represent a great alternative to the classic deterministic imaging techniques, that could require significant computational efforts. However, it exploits for its training a large amount of data and, for this specific application, the collection of a great number of measurements or numerical simulations can be a not easy task.

Here, we present an efficient method to generate simulations, to train ML algorithms, through the use of a linear integral operator with a significant reduction in time. The trained ML algorithm is the multilayer perceptron (MLP) [5] used then to classify brain strokes in terms of presence, type and position within the brain.

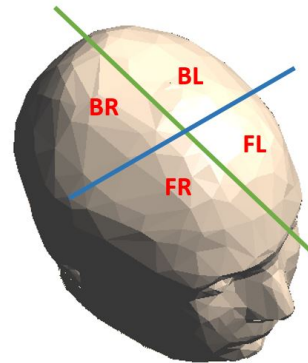


Fig. 1. Subdivision of the 3-D human head phantom in 4 regions: front left (FL), front right (FR), back left (BL) and back right (BR).

## II. DATA-SET GENERATION

The considered scenario is a head phantom wearing a helmet composed by 24 antennas, acting both as receiver and transmitter. The entire system is described in [6]–[8].

Considering, for each pair of antennas  $p$  and  $q$ , the angular frequency  $\omega = 2\pi f$ , the power waves  $a_p$  and  $a_q$  at the antennas ports, the dielectric complex permittivity of the average brain  $\epsilon_b$  (representing the healthy scenario), and the background fields  $\underline{E}_{b,p}$  and  $\underline{E}_{b,q}$  radiated by the two antennas, we can write a linear integral operator, obtained through the Born approximation [9], as:

$$\Delta S_{p,q} = -\frac{j\omega\epsilon_b}{2a_p a_q} \iiint_V \underline{E}_{b,p}(\underline{r}) \cdot \underline{E}_{b,q}(\underline{r}) \Delta\chi(\underline{r}) d^3\underline{r} \quad (1)$$

where “ $\cdot$ ” identifies a dot product between the background fields, and  $\underline{r}$  is the position vector in the domain of interest (DOI). The background field is the field radiated by each antenna in the healthy scenario, i.e. without the presence of the stroke.  $\Delta S_{p,q}$  is the differential scattering parameter at the  $p$  and  $q$  antennas ports corresponding to:

$$\Delta S_{p,q} = S_{p,q}^{tot} - S_{p,q}^{inc} \quad (2)$$

where  $S_{p,q}^{tot}$  and  $S_{p,q}^{inc}$  are the scattering parameters in the scenario under test and in the healthy one, respectively. Finally, the dielectric contrast  $\Delta\chi$  is defined as:

$$\Delta\chi(r) \triangleq \frac{\epsilon_r(r) - \epsilon_b(r)}{\epsilon_b(r)}, \quad (3)$$

where  $\epsilon_r$  is the dielectric complex permittivity of the stroke area. The linear integral operator in (1) allows to link together the differential scattering parameters at the antennas ports to the dielectric contrast within the brain and it is here used to generate the data-set.

The first step is the generation of  $\Delta\chi$  that is different from zero only in the stroke and its value depends on the type of stroke that can be ischemic or hemorrhagic. In this work, the stroke is represented by a sphere with a radius of  $1.5\text{ cm}$ , and different types of samples are created by moving the sphere randomly within the DOI. For the same stroke position, different noise levels are also added to generate more realistic dielectric contrast distributions. Then, applying the linear operator in (1) to each sample, the corresponding differential scattering parameters,  $\Delta S_{p,q}$ , are obtained for each antennas pair  $p$  and  $q$ . Finally,  $S_{p,q}^{inc}$  is summed to  $\Delta S_{p,q}$  to obtain  $S_{p,q}^{tot}$  that represents the machine learning input data. In particular, here, only the amplitude of the  $S_{p,q}^{tot}$  parameters are given in input to MLP to avoid to use phase data, in order to simplify the receiver architecture and lowering its cost.

The scattering matrix is symmetrical, so we consider as features only the amplitude of the superior triangular matrix. The total number of generated samples is 4500, almost equally distributed among the 9 classes. The classes are based on presence, typology (ischemic or hemorrhagic) and positions (four brain areas) of the stroke. Figure 1 shows the head subdivision in four areas: front left (FL), front right (FR), back left (BL) and back right (BR).

The code used to generate the whole data-set takes around 1 hour. The time to generate the same data-set via full-wave simulations using a finite element method (FEM) solver [10] would be 42 days.

### III. NUMERICAL RESULTS

The algorithm used to classify the samples is MLP. The data-set is divided into training set (80%) and test set (20%). The first step is the selection of hyper-parameters through the grid search method: this technique chooses the combination of hyper-parameters that optimizes a metric, in this case the highest accuracy. The MLP has 4 hidden layers with 1000, 500, 250 and 100 neurons, the activation function is the hyperbolic tangent function with a regularization term  $\alpha = 0.05$  and finally the solver for weight optimization is the stochastic gradient descent [5]. In Fig. 2, there is the normalized confusion matrix obtained through MLP, with in the rows the true labels and in the columns the predicted labels.

We can observe that the values on the principal diagonal (percentage of well-predicted samples for each class) are very close to 1; moreover the algorithm is able to completely distinguish the 3 macro-classes (healthy, ischemic and hemorrhagic stroke). The algorithm does not classify correctly the position of a few samples and it happens because, in these cases, the center of the sphere is very close to one of the head axes of

	N	I_FL	I_FR	I_BL	I_BR	H_FL	H_FR	H_BL	H_BR
N	1	0	0	0	0	0	0	0	0
I_FL	0	1	0	0	0	0	0	0	0
I_FR	0	0	1	0	0	0	0	0	0
I_BL	0	0.018	0	0.98	0	0	0	0	0
I_BR	0	0	0	0.013	0.99	0	0	0	0
H_FL	0	0	0	0	0	0.98	0	0.016	0
H_FR	0	0	0	0	0	0	0.99	0	0.012
H_BL	0	0	0	0	0	0	0	0.96	0.044
H_BR	0	0	0	0	0	0	0	0.0071	0.99

Fig. 2. MLP confusion matrix for linearized simulations. Yellow square for healthy cases (N), green square for ischemic stroke (I) and red square for hemorrhagic stroke (H). FL, FR, BL and BR distinguish the 4 regions of the head, see Fig. 1

symmetry and the stroke position is not well defined. We can evaluate the obtained classification performances through three metrics: accuracy, recall and precision, described in [11]. In our case, all these metrics assume values close to 1 for each class:  $accuracy > 0.99$ ,  $recall > 0.96$  and  $precision > 0.96$ .

Then, the trained algorithm is tested with some full-wave simulations obtained through a finite element method solver [10]. We create three full-wave simulations, one for each macro-class: a healthy case (class N), an ischemic stroke in the back-right head area (class I\_BR) and a hemorrhagic stroke in the back-left head area (class H\_BL). Then, each simulation is tripled adding white random noise three times, obtaining a testing set of 9 samples. In this case the algorithm correctly classifies all the samples, demonstrating that the MLP, trained via the linearized integral operator, can be successfully used to classify full-wave simulated data.

### IV. CONCLUSION AND PERSPECTIVES

In this paper, an innovative and fast method to generate a large data-set for machine algorithm training has been presented and applied for brain stroke classification, using amplitude data only. Under the Born approximation, the domain of scattering parameters is linked with the dielectric contrast domain through a linear integral operator allowing very fast simulations of the overall system. The results obtained in the classification with the MLP algorithm underlined a very high accuracy: the algorithm does not correctly classify the samples only in a few cases, i.e. when the stroke position is ambiguous, but it never missed the macro-class. Then, the MLP algorithm was tested with full-wave simulations, showing the capability to correctly classify all of them, and demonstrating that the proposed method to generate the training set is suitable for the classification of full-wave simulated data.

The next step is test the trained ML algorithm with measured scattering parameters, e.g. obtained with the microwave imaging system described in [7].

#### ACKNOWLEDGMENT

This work was supported by the MIUR under the PRIN project “MiBraScan”, and by the European Union’s Horizon 2020 Research and Innovation Program under the EMERALD project, grant agreement No. 764479.

#### REFERENCES

- [1] L. Crocco, I. Karanasiou, M. James, and R. C. Conceicao (Eds.), *Emerging Electromagnetic Technologies for Brain Diseases Diagnostics, Monitoring and Therapy*. Springer int. pub., 2018.
- [2] G. Zhu, A. Bialkowski, L. Guo, B. Mohammed, and A. Abbosh, “Stroke classification in simulated electromagnetic imaging using graph approaches,” *IEEE J. Electromagn., RF, Microw. Med. Biol.*, vol. 5, no. 1, pp. 46–53, 2021.
- [3] M. Salucci, A. Polo, and J. Vrba, “Multi-step learning-by-examples strategy for real-time brain stroke microwave scattering data inversion,” *Electronics*, vol. 10, no. 1, 2021.
- [4] M. Persson, A. Fhager, H. D. Trefna, Y. Yu, T. McKelvey, G. Pegenius, J.-E. Karlsson, and M. Elam, “Microwave-based stroke diagnosis making global prehospital thrombolytic treatment possible,” *IEEE Transactions on Biomedical Engineering*, vol. 61, no. 11, pp. 2806–2817, 2014.
- [5] M. A. Nielsen, *Neural Networks and Deep Learning*. 2019.
- [6] D. O. Rodriguez-Duarte, J. A. T. Vasquez, R. Scapaticci, L. Crocco, and F. Vipiana, “Brick-shaped antenna module for microwave brain imaging systems,” *IEEE Antennas Wireless Propag. Lett.*, vol. 19, no. 12, pp. 2057–2061, 2020.
- [7] J. A. Tobon Vasquez *et al.*, “A prototype microwave system for 3D brain stroke imaging,” *Sensors*, vol. 20, May 2020.
- [8] D. O. Rodriguez-Duarte, J. A. Tobon Vasquez, R. Scapaticci, G. Turvani, M. Cavagnaro, M. R. Casu, L. Crocco, and F. Vipiana, “Experimental validation of a microwave system for brain stroke 3-d imaging,” *Diagnostics*, vol. 11, no. 7, 2021.
- [9] R. Scapaticci, J. Tobon, G. Bellizzi, F. Vipiana, and L. Crocco, “Design and numerical characterization of a low-complexity microwave device for brain stroke monitoring,” *IEEE Transactions on Antennas and Propagation*, vol. 66, no. 12, pp. 7328–7338, 2018.
- [10] D. O. Rodriguez-Duarte, J. A. Tobon Vasquez, R. Scapaticci, L. Crocco, and F. Vipiana, “Assessing a microwave imaging system for brain stroke monitoring via high fidelity numerical modelling,” *IEEE J. Electromagn., RF, Microw. Med. Biol.*, pp. 1–1, 2021.
- [11] J. Davis and M. Goadrich, “The relationship between precision-recall and roc curves,” in *Proceedings of the 23rd International Conference on Machine Learning, ICML ’06*, (New York, NY, USA), p. 233–240, Association for Computing Machinery, 2006.